

# Mechanical characterization of pure Nb at cryogenic temperatures

M.S. Mahmood<sup>1,2</sup>, B.F. Beadle<sup>1,2</sup>, R. Laxminarayana<sup>3</sup>, E.D. Hintsala<sup>3</sup>, and A. Zare<sup>\*1,2</sup>

<sup>1</sup>School of Mechanical and Materials Engineering, Washington State University, Pullman, WA, USA

<sup>2</sup>Hydrogen Properties Energy Research Center, Washington State University, Pullman, WA, USA

<sup>3</sup>Bruker Nano Surfaces and Metrology, Eden Prairie, MN, USA

\*E-mail: arezoo.zare@wsu.edu

**Abstract.** The mechanical properties of commercially pure polycrystalline niobium were investigated in this study using nanoindentation and uniaxial tension over a temperature range from 77 K to room temperature. Both indentation hardness and yield strength were found to increase with decreasing temperature, accompanied by a transition from ductile necking to more brittle fracture. For samples tested under uniaxial tension at 77 K, the fracture surfaces were oriented at approximately 35 degrees relative to the loading direction. No evidence of cracking or localized shear banding was observed around the impressions made using nanoindentation. These findings provide insight into the mechanical behavior and deformation mechanisms of niobium at cryogenic temperatures and contribute to defining the safety limits of niobium components for low-temperature applications.

## 1. Introduction

Modern particle accelerators depend on superconducting radio-frequency (SRF) cavities to efficiently accelerate charged particles for research, medical applications, and isotope production. Niobium (Nb) is a desirable material for SRF cavities because of its high critical temperature (9.2 K), high critical magnetic field, and good machinability [1]. Because of its high ductility, Nb parts can be cold drawn from semi-finished to final geometries with high precision without the need for heat treatment [2]. In these applications, Nb must endure high-magnitude stresses and numerous loading cycles without failure, making its mechanical properties at both room and cryogenic temperatures critically important.

Mechanical properties of Nb are shown to be highly sensitive to temperature and purity. At room temperature, annealed Nb exhibits the yield point phenomenon, characterized by an initial stress peak followed by a sharp drop, rapid subsequent work hardening, and substantial ductility before failure. The Young's modulus of Nb is reported to be anisotropic along different crystallographic orientations [3,4]. At cryogenic temperatures, Nb shows a significant increase in both yield and tensile strength, accompanied by a reduction in ductility. For example, at liquid helium temperature (4.2 K), its tensile strength can reach up to five times that at room temperature. Similar findings have been reported from microscale mechanical testing of single crystal (001) Nb, where micropillars tested at 56 K and 100 K exhibited brittle behavior, including



early fracture and cleavage-like surfaces. In contrast, micropillars tested at room temperature deformed plastically, showing smooth stress-strain responses [5,6]. Although high-purity Nb (RRR 250 to 316) retains moderate ductility at cryogenic temperatures, commercially pure grades typically show a more brittle response and fail with minimal plastic deformation under the same loading conditions [7–10].

Considerable variations exist in the reported mechanical properties of Nb, primarily due to differences in purity levels, crystallographic orientations, and testing methodologies. Moreover, comparative studies between microscale mechanical behavior and bulk properties remain limited. The microstructural evolution and failure mechanisms of commercially pure Nb, particularly under cryogenic conditions, also remain inadequately understood. To address these gaps, this study employs nanoindentation and uniaxial tension tests on commercially pure Nb over a temperature range from 77 K to room temperature, offering new insights into its mechanical performance and deformation mechanisms.

## 2. Experimental Details

### 2.1 Material

A commercially pure Nb plate with dimensions of 12" × 3" × 0.24" was procured from Eagle Alloys Corporation (Talbot, TN, USA). The material conforms to the ASTM B393-18 [11] and is designated as R04210 Type 2 in an annealed condition. The elemental composition of the plate, provided by the manufacturer, is reported in Table 1.

**Table 1.** Elemental composition (in weight percent) of the commercially pure Nb material.

Elements	O	N	C	H	Ta	Mo	W
Results	0.0081	0.0007	0.0032	0.0003	0.0387	<0.0010	0.0027
Elements	Ti	Si	Fe	Hf	Zr	Ni	Nb
Results	0.0004	0.0001	0.0005	<0.0001	<0.0001	0.0004	Remainder

### 2.2 Nanoindentation Test

A Bruker TI 990 TriboIndenter equipped with the xSol Cryo setup was used to characterize Young's modulus and hardness of Nb across a temperature range of 178 – 303 K in 25 K increments. The experiments were performed using a nano Dynamic Mechanical Analysis (nanoDMA) low-load transducer and a diamond Berkovich indenter tip. To prepare specimens for nanoindentation, the Nb plate was sectioned to prismatic cubes with nominal dimensions of 7 mm × 7 mm × 4 mm. The prismatic specimens were then mechanically polished to a mirror-finish end using 600 and 1200 silicon carbide lapping films and diamond suspensions with particle sizes of 9, 6, 3, and 1 μm. An average surface roughness ( $R_a$ ) of 4.9 nm was measured on the polished samples using a scanning probe microscope (SPM), and the surface quality was further assessed through scanning electron microscopy (SEM). Figure 1 presents the corresponding SPM and SEM images captured prior to nanoindentation testing. According to ISO 14577 Annex E [12], surface roughness introduces uncertainty in contact area at shallow indentation depths due to asperity contact. At greater depths, this effect diminishes and can be represented as an uncertainty in indentation depth proportional to  $R_a$ . To keep this uncertainty below 5%, the contact depth should be at least 20 times  $R_a$ . In our case, the indentation depth used is much greater than  $20 \times R_a$ , so the visible scratches or surface deformations in Figure 1 are

not expected to affect the repeatability of the nanoindentation results. Indentations were carried out using a partial unload loading protocol within a load range of 200 to 10,000  $\mu\text{N}$ . At each temperature, 30 partial unloading steps were executed, and the test was repeated at six different locations.

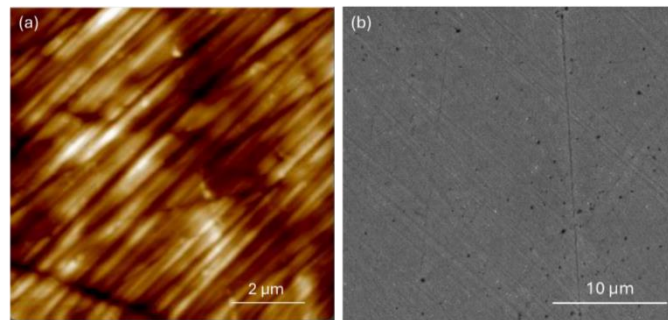


**Figure 1.** (a) SPM and (b) SEM images obtained from mechanically polished Nb surfaces.

### 2.3 Uniaxial Tensile Test

The Cryogenic Accelerated Fatigue Tester (CRAFT) [13], shown in Figure 2(a), was used to perform uniaxial tensile tests both at room temperature and 77 K. Mechanical loading was applied using an MTS Acumen 12 electrodynamic load frame, which can deliver static forces up to 8 kN and dynamic forces up to 12 kN, with a 70 mm actuator stroke and operating frequencies up to 100 Hz. A vacuum pressure of  $10^{-6}$  Torr was achieved inside the test chamber by sequential operation of an Agilent Varian IDP-07 scroll pump and a Varian TwisTorr 84-FS turbomolecular pump. Pressure was continuously monitored using a Varian FRG-70 inverted magnetron gauge. A Lakeshore 336 temperature controller with silicon diode sensors was used to measure and regulate testing temperature. To reduce thermal radiation into the test chamber, a multi-layer insulation system and an actively cooled copper shield were employed. Cryogenic cooling was provided by a Cryomech PT415 pulse tube cryocooler, delivering 19 W of cooling at 20 K. The test chamber, with an internal diameter of 57.15 mm and a height of 228.6 mm, accommodated specimens conforming to ASTM D638 [14] as illustrated in Figure 3(a). The specimens were machined using a water jet cutter and then lightly polished to remove surface asperities caused by the cutting grips and to minimize potential stress concentration sites. Custom-designed grips and dowel pins were employed to maintain a secure grip on the specimens throughout testing. Uniaxial tension tests were conducted at a displacement rate of 0.1 mm/s for the first trial and 0.03 mm/s for the second trial, with strain estimated based on the actuator displacement.

To investigate the effect of specimen length scale, larger specimens conforming to ASTM E466 [15] were tested using an Instron 2716-003 tensile testing machine, as shown in Figure 2(b) and Figure 3(b). The larger specimens were tested exclusively at room temperature under a displacement rate of 0.03 mm/s, with displacement measured using an extensometer. Overall, two samples were tested under uniaxial tension at room temperature, and two samples at 77 K.



**Figure 2.** (a) Cryogenic Accelerated Fatigue Tester (CRAFT) setup, and (b) Instron 2716-003 tensile testing machine.

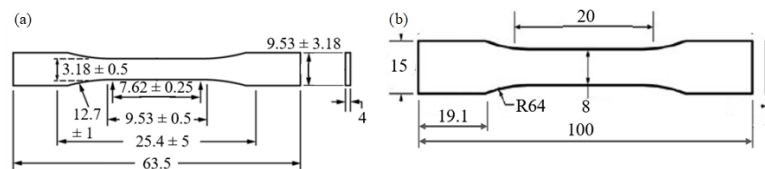


**Figure 3.** Geometry and dimensions (in mm) for (a) ASTM D638 and (b) ASTM E466 specimens.

### 3. Results and Discussion

#### 3.1 Nanoindentation Results

Figure 4 shows a typical load ( $P$ ) vs. displacement ( $h$ ) curve obtained from testing Nb at room temperature. The curve shows 30 sequential loading and hold steps followed by partial unloading. The data enables the evaluation of reduced elastic modulus ( $E_r$ ) and hardness ( $H$ ) using the procedure of Oliver and Pharr [16]. The initial stage of each unloading segment was fit to a power law which then allowed for the determination of the stiffness during unloading ( $S=dP/dh$ ), and the contact area ( $A$ ) at the applied force,  $P_{max}$ . The reduced elastic modulus and hardness were then obtained by  $E_r = \pi^{1/2}S/(2A^{1/2})$  and  $H = P_{max}/A$ . Subsequently, the reduced elastic modulus was converted to Young's modulus ( $E$ ) using  $1/E_r = (1-\nu^2)/E + (1-\nu_i^2)/E_i$ , where  $\nu$  is the Poisson's ratio of the specimen (0.397),  $\nu_i$  is the Poisson's ratio of the indenter (0.07), and  $E_i$  is the Young's modulus of the indenter (1,141 GPa).

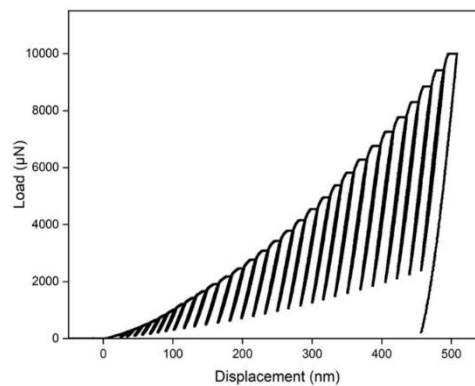


**Figure 4.** Load vs. displacement curve for Berkovich indentations performed on Nb at room temperature.

Figure 5 shows the values of Young's modulus and hardness of Nb as a function of indentation contact depth ( $h_c$ ) across all tested temperatures. Both properties decrease with increasing

contact depth and approach a near-plateau region beyond 100 to 200 nm. The apparent decrease in hardness and modulus below 100 nm is primarily due to tip area calibration errors, likely originating from the indenter tip's rounded geometry dominating at shallow depths rather than the ideal pyramidal shape. Overall, the highest values of Young's modulus and hardness were recorded at the testing temperature of 203 K. Evidence of icing was observed on the sample surface at 178 K, which may account for the increased measurement variability.

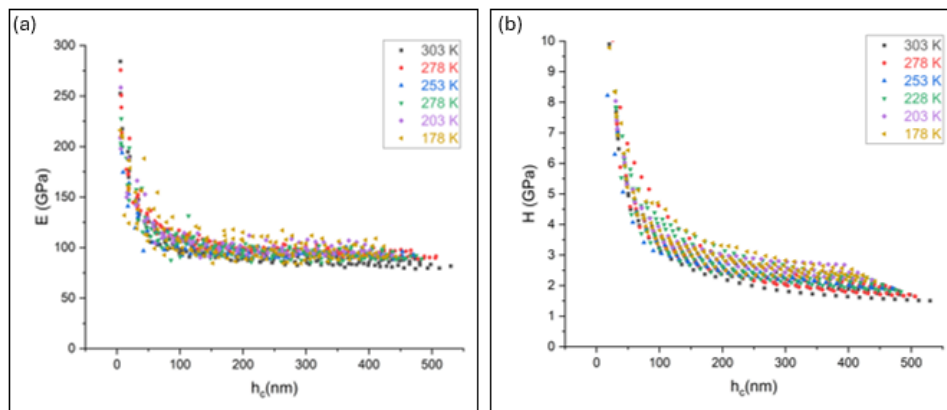


**Figure 5.** (a) Elastic modulus vs. contact depth curve, (b) Hardness vs. contact depth at a temperature range of 153 – 303 K.

To better establish trends in mechanical behavior, the values of Young's modulus and hardness were averaged over an indentation contact depth range of 300 to 400 nm. The resulting average values are presented as box plots in Figure 6. The average values of Young's modulus fluctuate as temperature decreases, without exhibiting a consistent trend, and show greater variability at lower temperatures. As previously noted, this increased variability is attributed to icing on the specimen surface. In contrast, the average hardness values exhibit a clear monotonic increase as the temperature decreases from 303 K to 178 K, indicating a pronounced temperature dependence of the material's resistance to localized plastic deformation. The increase in hardness is postulated to result from reduced atomic mobility at lower temperatures, which limits dislocation motion and thereby enhances resistance to plastic deformation. Uniaxial tensile tests also demonstrated an increase in yield strength and strain hardening rate, along with a reduction in ductility, at 77 K compared to room temperature. These results are consistent with thermally activated deformation mechanisms commonly observed in metals, which contribute to increased strength and decreased ductility at cryogenic temperatures.

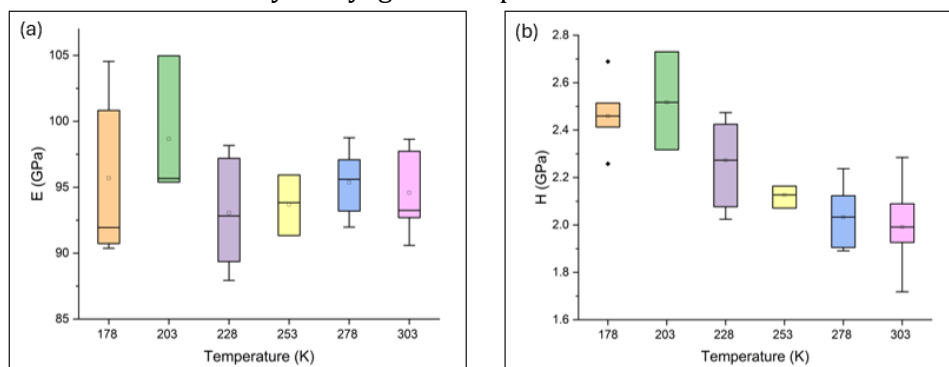


**Figure 6.** Box plots showing the average values of (a) Young's modulus and (b) hardness of Nb obtained from nanoindentation experiments at 178 – 303 K.

### 3.2 Uniaxial Tension Results

Figure 7 shows the stress-time curves obtained from both tested specimen geometries (ASTM D638 and ASTM E466) at room temperature or 77 K. The yield strength was determined from the stress-time response obtained during monotonic loading at a constant strain rate. Because strain increases linearly with time under constant strain-rate conditions, the stress-time plot can be directly interpreted in a manner analogous to a stress-strain curve. The elastic region was identified as the initial linear portion of the curve, and the yield point was taken as the stress corresponding to the first measurable deviation from linearity. For improved accuracy, the conventional 0.2% offset method was applied by converting time to strain using the imposed strain rate, constructing a line parallel to the elastic slope with a 0.2% strain offset, and locating its intersection with the stress-time curve. The stress at this intersection was reported as the yield strength.

At room temperature, the ASTM E466 specimen exhibits a yield strength of ~200 MPa and an ultimate tensile strength of 241 MPa. The total elongation, measured using an extensometer, was 5.4 mm which corresponds to a total longitudinal strain of 0.27. The smaller ASTM D638 specimen shows a comparable yield strength of 205 MPa and a slightly higher ultimate tensile strength of 253 MPa, suggesting that size effects are negligible for the specimen dimensions tested in this study. The two ASTM D638 specimens tested at 77 K exhibit an increase in both yield strength and strain hardening rate compared to their room temperature counterpart. This trend is consistent with previous studies that have reported an increase in the strength of Nb as the temperature decreases [10]. A comparison of yield and ultimate tensile strength values obtained in this study with those reported in prior work is provided in Table 2. We note here that significant variations were observed in the stress-strain responses of the specimens tested at 77 K, suggesting potential inconsistencies in the testing protocols. Additionally, the larger strain values recorded for the ASTM D638 specimens are likely an artifact resulting from reliance on actuator displacement data rather than direct measurements. Efforts are currently underway to reduce the inconsistencies and conduct additional measurements to establish clear trends.

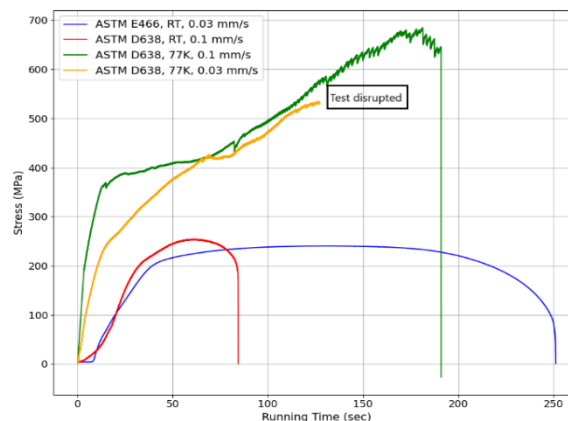


**Figure 7.** Stress-time curves of Nb under uniaxial tension at room temperature and 77 K. Displacement for ASTM E466 and D638 tests were recorded using an extensometer and actuator displacement, respectively.



**Table 2.** Tensile properties of Nb obtained in this study compared with values reported in the literature.

Material	Displacement Rate (mm/s)	Temperature (K)	Yield Strength (MPa)	Ultimate Tensile strength (MPa)	Reference
Nb, RRR 250	Not mentioned	77	~600	~650	Compton et al. [9]
Nb, RRR 250	0.0083 mm/s	77	618	642	Walsh et al. [10]
Nb, RRR 40	0.0083 mm/s	77	443	502	Walsh et al. [10]
Nb, Commercially pure (ASTM D638)	0.1 mm/s	77	368	~683	Present study
Nb, Commercially pure (ASTM D638)	0.03 mm/s	77	245	-	Present study
Nb, RRR 250	0.0083 mm/s	295	70	151	Walsh et al. [10]
Nb, RRR~40	0.0083 mm/s	295	76	171	Walsh et al. [10]
Nb, RRR~306	0.2 mm/s	298	117	189	Wu et al. [17]
Nb, Commercially pure (ASTM E466)	0.03 mm/s	298	205	253	Present study
Nb, Commercially pure (ASTM D638)	0.1 mm/s	298	200	241	Present study

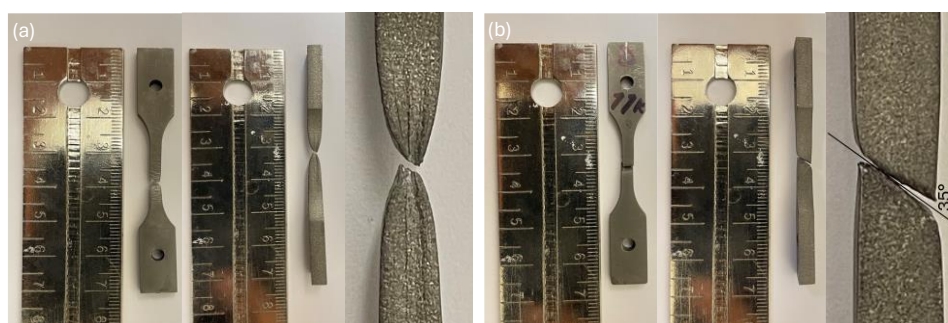
**Figure 8.** Fractured ASTM D638 specimens after uniaxial tension at (a) room temperature and (b) 77 K.

Figure 8 shows the fracture surfaces of ASTM D638 specimens tested at room temperature and 77 K. At room temperature, the specimen exhibits significant necking prior to failure, characteristic of ductile behavior. In contrast, the specimen tested at 77 K shows minimal necking, and the fracture surfaces are inclined at approximately 35° to the loading axis, indicating a more brittle fracture mode.

#### 4. Summary and Conclusion

The mechanical response of commercially pure niobium (Nb) was investigated using nanoindentation over a temperature range of 178 K to 303 K, along with uniaxial tensile tests conducted at room temperature and 77 K. Nanoindentation results revealed a monotonic increase in hardness with decreasing temperature up to 203 K, while Young's modulus remained relatively unchanged across the tested temperature range. A transition toward a more brittle response between room temperature and 77 K was evidenced by both uniaxial tensile testing and post-mortem analysis of the fracture surfaces.

#### Acknowledgments

Funding for the project was provided by the Fermilab and Washington State University, School of Mechanical and Materials Engineering. Guidance from Prof. Jacob Leachman on cryogenic measurements is gratefully acknowledged.

#### References

- [1] Padamsee H, Knobloch J and Hays T 2008 *RF Superconductivity for Accelerators* (John Wiley & Sons).
- [2] Spitzig W A, Trybus C L and Laabs F C 1991 Structure properties of heavily cold-drawn niobium *Materials Science and Engineering: A* **145** 179–87.
- [3] Antoine C, Foley M and Dhanaraj N 2011 *Physical Properties of Niobium and Specifications for Fabrication of Superconducting Cavities* (Fermi National Accelerator Lab. (FNAL), Batavia, IL (United States)).
- [4] Kim M, Chen K, Carriere P, Matavalam N, Penney J, Kutsaev S and Korkolis Y P 2022 Mechanical behavior and forming of commercially-pure niobium sheet *International Journal of Solids and Structures* **257** 111770.
- [5] Song G, Aragon N K, Ryu I and Lee S 2021 Low-temperature failure mechanism of [001] niobium micropillars under uniaxial tension *Journal of Materials Research* **36** 2371–82.
- [6] Lee S-W, Cheng Y, Ryu I and Greer J R 2014 Cold-temperature deformation of nano-sized tungsten and niobium as revealed by in-situ nano-mechanical experiments *Sci. China Technol. Sci.* **57** 652–62.
- [7] Ciovati G, Dhakal P, Matalovich J, Myneni G, Schmidt A, Iversen J, Matheisen A and Singer W 2015 Mechanical properties of niobium radio-frequency cavities *Materials Science and Engineering: A* **642** 117–27.
- [8] M. Hörmann 1993 Mechanical Properties of Nb 100 at Cryogenic Temperatures (4.2 K) *High Temperature Materials and Processes* **11** 139–58.
- [9] Compton C, Chandrasekaran S K, Baars D, Bieler T, Darbandi P and Wright N 2010 Development of A Cryogenic Mechanical Property Testing Station for Superconducting Rf Cavity Material *AIP Conference Proceedings* **1218** 587–94.
- [10] Walsh R P, Mitchell R R, Toplosky V T and Gentzlinger R C, *Low Temperature Tensile and Fracture Toughness Properties of SRF Cavity Structural Materials*, Proc. of the SRF99, Santa Fe, NM, USA (1999).
- [11] ASTM International 2018 *ASTM B393-18: Standard Specification for Niobium and Niobium Alloy Strip, Sheet, and Plate* (West Conshohocken, PA: ASTM International).
- [12] ISO 14577-1:2015(en), Metallic materials — Instrumented indentation test for hardness and materials parameters — Part 1: Test method
- [13] Hunt M A 2021 Cryogenic Accelerated Fatigue Tester for Characterization of 3d-Printed Polymer Matrix Composites.
- [14] ASTM D638-22 2022 *Standard Test Method for Tensile Properties of Plastics* (West Conshohocken, PA: ASTM International).
- [15] ASTM E466-21 2021 *Standard Practice for Conducting Force Controlled Constant Amplitude Axial Fatigue Tests of Metallic Materials* (West Conshohocken, PA: ASTM International).
- [16] Oliver W C and Pharr G M 1992 An improved technique for determining hardness and elastic modulus using load and displacement sensing indentation experiments *Journal of Materials Research* **7** 1564–83.
- [17] Wu G, Dhanaraj N, Cooley L, Hicks D, Hahn E, Burk D, Muranyi W, Foley N, Edwards H, Harms E and Champion M 2009 *Tensile tests of niobium material for SRF cavities* (Fermi National Accelerator Lab. (FNAL), Batavia, IL (United States)).